the conditions used here (*6*, *28*). It has been proposed that a change in the oxidation potential of the gas may change the oxygen content in the ZnO surface and thereby the interface energy (*6*, *7*, *28*). A low oxygen content will give a strong decrease in the Cu/ZnO_x interface energy because of a partial (or full) reduction of the ZnO surface layer. On the other hand, at large oxygen contents, the ZnO surface is completely oxidized (low concentration of oxygen vacancies) and the interface free energy is high.

Previously, detailed information on gas-induced structural transformation has been obtained with single-crystal model systems exposed to conditions quite far removed from those used in industrial catalysis. Thus, it has been difficult to relate the information directly to catalysis, and this has been referred to as the material and pressure gaps in catalysis (*16*). Our results show that insight can now be obtained at more realistic conditions and for quite complex nanoparticle systems with many different surfaces and interfaces. The observed dynamic restructuring of the catalyst also demonstrates that the relevant active sites are generated during the catalytic reaction. This further emphasizes the need for in situ studies at all the conditions that a catalyst will experience. Such studies may provide important information regarding the concentration of different type of surface sites (on low index planes, corners, steps, etc.) under various conditions (*36*). The structure sensitivity and dynamic morphology changes may then be incorporated into a microkinetic description of the catalytic reactions with the approach discussed earlier (*28*). Previously descriptions of catalysis have had to rely on assumptions regarding the nature of the exposed surfaces.

References and Notes

1. M. A. El-Sayed, *Acc. Chem. Res.* **34**, 257 (2001).
2. G. Ertl, H. Knözinger, J. Weitkamp, Eds., *Handbook of Heterogeneous Catalysis* (Wiley-VCH, New York, 1997), vol. 4, pp. 1856–1876.
3. A. P. Alivisatos, *Science* **271**, 933 (1996).
4. R. Jin *et al.*, *Science* **294**, 1901 (2001).
5. J. A. Dumesic, H. Topsøe, M. Boudart, *J. Catal.* **37**, 513 (1975).
6. B. S. Clausen *et al.*, *Top. Catal.* **1**, 367 (1994).
7. J. D. Grunwaldt, A. M. Molenbroek, N.-Y. Topsøe, H. Topsøe, B. S. Clausen, *J. Catal.* **194**, 452 (2000).
8. M. M. Günther *et al.*, *Catal. Lett.* **71**, 37 (2001).
9. T. W. Hansen *et al.*, *Science* **294**, 1508 (2001).
10. J. A. Dumesic, H. Topsøe, *Adv. Catal.* **26**, 121 (1977).
11. B. S. Clausen, H. Topsøe, R. Frahm, *Adv. Catal.* **42**, 315 (1998).
12. J. M. Thomas, G. A. Somorjai, Eds., *Topics in Catalysis*, vol. 8 (Balzer Science Publishers BV, Bussum, the Netherlands, 1999).
13. G. A. Somorjai, *Cattech* **3**, 84 (1999).
14. J. W. Niemantsverdriet, *Spectroscopy in Catalysis* (Wiley-VCH, Weinheim, Germany, 2000).
15. C. T. Campbell, *Science* **294**, 1471 (2001).
16. N. I. Jaeger, *Science* **293**, 1601 (2001).
17. D. A. Jefferson, P. J. F. Harris, *Nature* **332**, 617 (1988).
18. R. M. Stockman, H. W. Zandbergen, A. D. Langeveld, J. A. Moulijn, *J. Mol. Catal. A Chem.* **102**, 147 (1995).
19. J. Urban, H. Sack-Kongehl, K. Weiss, *Catal. Lett.* **49**, 101 (1997).
20. A. K. Datye, in *Handbook of Heterogeneous Catalysis*, G. Ertl, H. Knözinger, J. Weitkamp, Eds. (Wiley-VCH, New York, 1997), vol. 2, pp. 493–512.
21. J. M. Thomas, *Angew. Chem. Int. Ed.* **38**, 3588 (1999).
22. R. T. Baker, P. S. Harris, *J. Phys. E Sci. Instrum.* **5** (no. 8), 793 (1970).
23. P. L. Gai, E. Boyes, *Ultramicroscopy* **67**, 219 (1997).
24. J. B. Hansen, in *Handbook of Heterogeneous Catalysis*, G. Ertl, H. Knözinger, J. Weitkamp, Eds. (Wiley-VCH, New York, 1997), vol. 4, pp. 1856–1876.
25. J. R. Rostrup-Nielsen, *Phys. Chem. Chem. Phys.* **3**, 283 (2001).
26. N.-Y. Topsøe, H. Topsøe, *J. Mol. Catal. A Chem.* **141**, 95 (1999).
27. F. Boccuzzi, G. Ghiotti, A. Chiorino, *Surf. Sci.* **156**, 933 (1985).
28. C. V. Ovesen *et al.*, *J. Catal.* **168**, 133 (1997).
29. The ZnO support was prepared by flame synthesis in order to obtain well-developed crystals (*37*). Stöber spheres of diameter 600 to 700 nm were used as silica support (*38*). After impregnation and drying, the catalysts were heated in 2% O_2 in N_2 at 400°C for 4 hours.
30. C. R. Henry, *Surf. Sci. Rep.* **31**, 231 (1998).
31. K. H. Hansen *et al.*, *Phys. Rev. Lett.* **83**, 4120 (1999).
32. G. Wulff, *Z. Kristallogr.* **34**, 449 (1901).
33. P. Stadelmann, *Ultramicroscopy* **21**, 131 (1987).
34. S. Bernal *et al.*, *Ultramicroscopy* **72**, 135 (1998).
35. C. T. Campbell, *Surf. Sci. Rep.* **27**, 1 (1997).
36. J. B. Wagner, P. L. Hansen, S. Helveg, B. S. Clausen, N.-Y. Topsøe, H. Topsøe, in preparation.
37. J. R. Jensen, T. Johannesen, S. Wedel, H. Livbjerg, *J. Nanoparticle Res.* **2** (no. 4), 363 (2000).
38. W. Stöber, A. Fink, E. Bohn, *J. Colloid Interface Sci.* **26**, 82 (1968).
39. L. Vitos, A. V. Ruban, H. L. Skriver, J. Kollár, *Surf. Sci.* **411**, 186 (1998).
40. We would like to thank K. Højrup Hansen, E. Johnson, C. V. Ovesen, A. Datye, and N.-Y. Topsøe for fruitful discussions; T. Johannesen for supply of the flame-synthesized ZnO[37]; and H. Teunissen for preparation of the catalysts. Haldor Topsøe, H.-J. Hansen, and W. T. Liu are gratefully acknowledged for keen interest in the establishment of the microscope facility, and the China Technical Consultants Foundation is thanked for financial participation. J.B.W. would like to thank the Danish Research Academy for supporting a scholarship at the Interdisciplinary Center of Catalysis (ICAT). S.H. acknowledges support from the Danish Research Council, STVF, through an extension of its materials development program. The FEI company is thanked for fruitful collaboration on the development of the in situ TEM.

26 December 2001; accepted 14 February 2002

Lateral Hopping of Molecules Induced by Excitation of Internal Vibration Mode

T. Komeda,[1] Y. Kim,[1] Maki Kawai,[1]* B. N. J. Persson,[2] H. Ueba[3]

We demonstrate electron-stimulated migration for carbon monoxide (CO) molecules adsorbed on the Pd(110) surface, which is initiated by the excitation of a high-frequency (HF) vibrational mode (C–O stretching mode) with inelastic tunneling electrons from the tip of scanning tunneling microscopy. The hopping phenomenon, however, cannot be detected for CO/Cu(110), even though the hopping barrier is lower than in the CO/Pd(110) case. A theoretical model, which is based on the anharmonic coupling between low-frequency modes (the hindered-translational mode related to the lateral hopping) and the HF mode combined with electron-hole pair excitation, can explain why the hopping of CO is observed on Pd(110) but not on Cu(110).

The diffusion of adsorbed species on surfaces can be controlled thermally to some extent. The nonthermal control of surface migration of adsorbates (using electron excitation) could have many applications. Only a few studies have shown that electron irradiation can induce nonthermal transfer of surface species (*1*, *2*), a process called electron-stimulated migration (ESM). Atoms can be manipulated with the scanning tunneling microscope (STM) (*3*), and excitation of the adsorbate-substrate vibrational mode induces various surface phenomena such as desorption (*4*), dissociation (*5*), and rotation of adsorbates (*6*). For example, the rotation of C_2H_2 on Cu is enhanced with the excitation of C–H stretching vibrational mode (*7*). However, the detailed mechanism of the coupling between the rotation of the molecule and the vibrational mode is still an open question. Here, we demonstrate ESM caused by tunneling electrons for CO molecules adsorbed on Pd(110), which is initiated by the excitation of a high-frequency (HF) vibrational mode (C–O stretching mode, ~240 meV). The hopping phenomenon, however, cannot be detected for CO/Cu(110) in spite of the much lower hopping barrier than for CO/Pd(110). The underlying mechanism is examined by a theoretical calculation that includes anharmonic coupling between low-frequency (LF, ~25 meV) modes (the hindered-translational mode related to the lateral hopping) and the HF mode, as well as the vibrational damping of the HF mode caused by electron-

---

[1] RIKEN, 2-1 Hirosawa, Wako, Saitama, 351-0198, Japan. [2] IFF, FZ-Jülich, 52425, Jülich, Germany. [3] Department of Electronics, Toyama University, Gofuku, Toyama, Japan.

*To whom correspondence should be addressed. E-mail: maki@postman.riken.go.jp

hole pair (EHP) excitation. The theory explains why hopping of CO is observed on Pd(110) but not on Cu(110) (*8, 9*).

When a certain amount of tunneling current is dosed to an isolated CO molecule on Pd(110), lateral motion of the molecule along the $[1\bar{1}0]$ direction is induced with a certain probability. Thermal hopping was negligible at the temperature used (4.8 K), and scanning the STM tip under normal tunneling conditions (typically sample bias voltage $V_s = 100$ mV and tunneling current $I_{tunnel} = 1$ nA) causes no change of the adsorption site of CO. Four CO molecules are apparent in Fig. 1A as white protrusions; CO adsorbs at the bridge site on Pd(110) (*10*). The molecule marked "a" in Fig. 1A was then dosed with tunneling electrons for 1 s at $V_s = 350$ mV and $I_{tunnel} = 7$ nA. Further imaging revealed that molecule "a" has jumped three Pd lattice spacing to the left along the $[1\bar{1}0]$ direction (Fig. 1B), but no change was seen in the bonding position of other molecules such as molecule "b."

The lateral hopping of CO was anisotropic and restricted to the $[1\bar{1}0]$ direction along the Pd rows on the Pd(110) surface. Taking advantage of this observation, we used the following method in addition to conventional two-dimensional (2D) imaging to visualize the hopping of molecules and to significantly increase the sampling number. The scanning of the STM tip was restricted to a single Pd row along $[1\bar{1}0]$, alternately repeating tunneling current injection on an adsorbate and STM observation with several 1D scanning. The *y* axis in the image created by this method corresponds to the passage of time, and the *x* axis indicates the position in space. Hereafter, we call this procedure the "1D dose-and-scan method." A similar measurement technique for step-kinetic investigation has been reported by Kitamura *et al.* (*11*).

We applied the dose-and-scan method to CO/Pd(110) for the cases of $V_s = 200$ mV (Fig. 1C) and 300 mV (Fig. 1D). The tunneling electrons were dosed for 1 s with a current of 7 nA, and 48 cycles of the dose-and-scan sequence were repeated in the image. At $V_s = 200$ mV, the adsorbate feature shows only a straight line, indicating that no lateral motion was induced and that the thermal drift was negligible. At $V_s = 300$ mV, the CO molecule hopped stochastically to the nearest-neighbor bridge site.

We measured the hopping probability as a function of V_s (*12*). The result is shown in Fig. 2A for V_s up to 550 mV. The probability shows a sharp increase beyond a threshold voltage between 200 and 300 mV. The behavior near the threshold is shown in detail in Fig. 2B both for the normal CO and $C^{13}O^{16}$ molecules, in which the *y* axis corresponds to the hopping probability per tunneling electron expressed in log-scale. In addition, the slope of the probability curve is shown in Fig. 2C. The probability shows a small but clear isotope shift, and the threshold energy can be assigned from Fig. 2C at 240 and 235 meV for the normal CO and $C^{13}O^{16}$, respectively. We note that the excitation energy of the C–O stretching vibrational mode is very close to the threshold voltage of 240 mV (*13*), and the isotope shift of 5 meV to lower energy in the threshold energy is a reasonable value for $C^{13}O^{16}$ (*14*). In addition, the slope of the hopping probability expressed in log-scale falls off with a narrow energy width. These findings suggest the involvement of C–O stretching excitation in the hopping of CO.

The hopping probability varied linearly as a function of the number of dosed tunneling electrons at fixed $V_s = 350$ mV (Fig. 2D). Hopping appears to be induced by the tunneling current, which would exclude other mechanisms, such as coupling between the molecular dipole moment and the electric field formed by the STM tip. Also, the linear increase of the hopping probability shows that this is a single-electron event instead of a multiple-electron effect. This result is expected theoretically, because the strong damping of the hindered-translational mode related to the hopping inhibits the ladder climbing process. We estimate that 5.4×10^{10} electrons are required to induce a single hopping event (*15*).

We have performed the same experiments as described above for CO/Cu(110). The result shows that the hopping probability for CO on Cu(110) under the same conditions as in Fig. 2A is less than 0.01 for V_s up to 550 meV; almost no lateral hopping is induced on CO/Cu(110) under the current setting. The diffusion barrier for CO on Cu(110) has been estimated to be ~97 meV (*16*), which is considerably lower than ~180 meV for CO on Pd(110). Also, we cannot expect a large difference in the excitation probability of the C–O stretching mode between CO/Pd(110) and CO/Cu(110).

The results so far described indicate that the excitation of the HF vibrational mode by tunneling electrons induces lateral hopping of CO on Pd(110). How is the excitation of the HF mode related to lateral hopping, and why

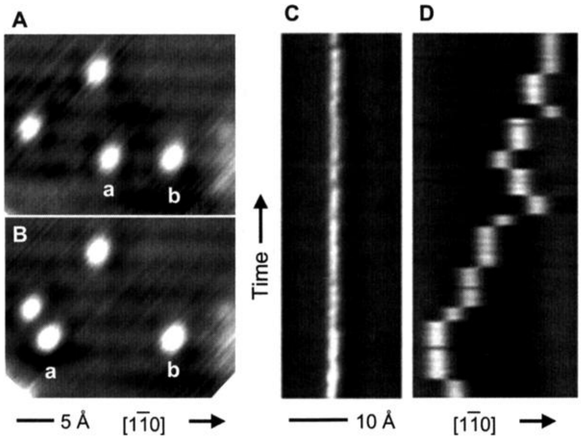

Fig. 1. (**A** and **B**) STM images (31 Å by 25 Å, $I_{tunnel} = 1$ nA, $V_s = 50$ mV) of four CO molecules on Pd(110). Images are (A) before and (B) after dosing tunneling electrons on the target molecule "a." (**C** and **D**) One-dimensional dose-and-scan method images for an isolated CO on Pd(110). Sample bias voltage for electron dosing is (C) 200 mV and (D) 300 mV. Totally 48 sequences are executed on both cases. Anisotropic hopping along the $[1\bar{1}0]$ direction with a unit of Pd lattice (2.75 Å) is clearly visible in the right panel.

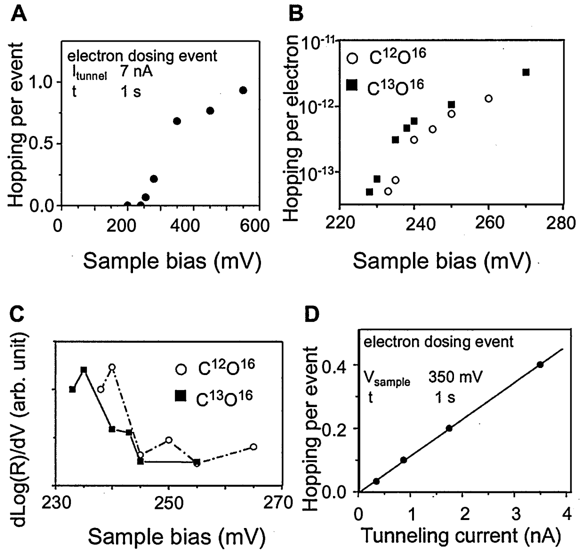

Fig. 2. (**A**) The hopping probability as a function of the bias voltage of dosed tunneling electrons ($I_{tunnel} = 7$ nA, 1 s) examined for CO on Pd(110) surface. (**B**) Expanded around $V_s = 240$ mV; the *y* axis is shown in log-scale and corresponds to the probability per electron. (**C**) The slope of the data in (B). (**D**) The hopping probability as a function of the tunneling current with the sample bias voltage of 350 mV. The linear line corresponds to the result of the least-squares fitting.

is it absent for CO on Cu(110) in spite of its much lower hopping barrier? We now examine these issues through theoretical calculations for CO/Pd(110) and CO/Cu(110).

We briefly describe a new theory of how the excitation of the HF mode can induce dynamical motion of adsorbates on metal surfaces (*17*). The probability of adsorbate rearrangements following the vibrational excitation of the HF mode Ω is calculated with a model that includes vibrational relaxation via EHP excitation, and anharmonic coupling $\delta\omega$ to the LF mode ω_0 associated with the relevant reaction coordinate.

The adsorbate is initially localized at the bottom of a potential well $U(v)$, and we assume that $U(v)$, in the region of v-space probed by the adsorbate when it is in its ground state ψ_0, can be approximated as harmonic $U(v) \approx m\omega_0^2v^2/2$ (*18*). We will refer to vibrations in this potential well as the LF mode ω_0. Adsorbate transfer from one well to another requires the transition of a barrier of height ε_B (Fig. 3A). If the interaction hamiltonian between the HF mode Ω (normal-mode coordinate u) and the reaction coordinate v is expanded to second-order in u, then $H_{int} = U_1(v)u + U_2(v)u^2$. The first term of H_{int} allows the HF mode of the molecule to decay by exciting the motion along the reaction coordinate v. If $\hbar\Omega \gg \varepsilon_B$, energy conservation requires that the molecule be excited to a continuum state ψ_k far above the potential barrier ε_B (Fig. 3B). However, because of the rapid oscillations in the wavefunction ψ_k, the matrix element $<\psi_k| U_1(v)|\psi_0>$ is extremely small. If $(\hbar\Omega - \varepsilon_B)/\hbar\omega_0 \gg 1$, a second-order process involving the excitation of the adsorbate to a level immediately above the barrier ε_B, with the rest of the energy $\approx \hbar\Omega - \varepsilon_B$ used to create an EHP excitation, has a higher probability (Fig. 3C). Because the final state has no HF excitation, this second-order process is only possible when the term $U_2(v)u^2$ is involved, rather than the term $U_1(v)u$.

We first consider the first-order process in which the molecule is excited from the initial state (the HF mode in the excited state; the LF mode in the ground state) to the final state (the HF mode in the ground state; the LF mode in the continuum state above the top of the potential barrier of the height ε_B). The HF mode decays by exciting the LF mode to a level above the potential barrier. We approximately obtain (*17*)

$$w_1 \approx \frac{\varepsilon^*}{\hbar}\left(\frac{\hbar\delta\omega}{\hbar\omega_0}\right)^2 n_0^{1/2}e^{-2n_0} \qquad (1)$$

where $n_0 = \Omega/\omega_0$, and where ε^* is of the order of the dissociation energy (or bond-breaking energy) associated with the HF mode.

Next, let us consider a second-order process in the presence of the vibrational damping caused by EHP excitation. We calculate the transition probability from the initial state (the HF mode in the excited state, the LF mode in the ground state, and no EHP excited) to the final state (the HF mode in the ground state, the LF mode in a continuum state above the top of the potential barrier, and an EHP excited). The transition rate for the adsorbate to be excited to a level immediately above the barrier, with the rest of the energy $\approx\hbar\Omega - \varepsilon_B$ transferred to an EHP excitation can be approximately obtained as (*17*)

$$w_2 \approx w_{ch}\left(\frac{\hbar\delta\omega}{\varepsilon_B}\right)^2\left(1-\frac{\varepsilon_B}{\hbar\Omega}\right)n^{3/2}e^{-2n} \qquad (2)$$

where $n = \varepsilon_B/\hbar\omega_0$ and w_{ch} is the vibrational damping rate of the HF mode Ω caused by excitation of an EHP.

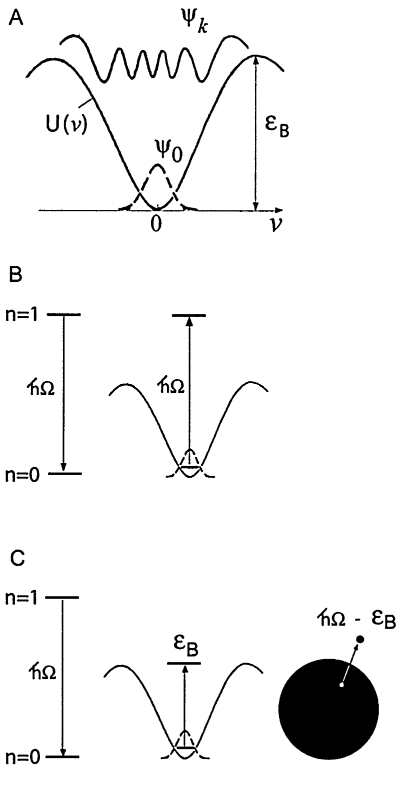

Fig. 3. (**A**) The potential energy $U(v)$ associated with the reaction coordinate v. The diffusion barrier ε_B and the ground state ψ_0 and excited ψ_k wave functions are indicated. (**B**) First-order process leading to hopping. The energy $\hbar\Omega$ of the HF mode is completely transferred to the reaction coordinate mode, which is excited to a state well above the top of the diffusion barrier ε_B. (**C**) A second-order process where the energy of the HF mode is transferred partly to the reaction coordinate mode, which is excited to a state just above the top of the diffusion barrier, whereas the rest of the energy is deposited as an electron-hole pair. The black circle denotes the Fermi sphere of the metal. When $(\hbar\Omega - \varepsilon_B)/\hbar\omega_0 \gg 1$ [where ω_0 is the frequency of small-amplitude vibrations in the potential well $U(v)$], process (C) will dominate over process (B).

Because the dominant channel of vibrational relaxation of HF modes is through EHP excitation for adsorbates on metals, $P = w_2/w_{ch}$ (and w_1/w_{ch}) can be interpreted as the fraction of the vibrational excited molecules which decay by transferring enough energy to the reaction coordinate to overcome the potential barrier via the second-order (and first-order) process. The anharmonic coupling of the HF mode to the LF mode is estimated to be $\hbar\delta\omega \sim -0.18$ meV for CO/Cu(100) (*19*). A similar value of $\hbar\delta\omega$ is expected for CO/Cu(110) because it has the same on-top adsorption site. Although no anharmonicity data are available for the CO/Pd system, $\hbar\delta\omega$ has been estimated at ~4.3 meV for CO/Ni(111) (*20, 21*). On the basis of the similarity of the bonding configuration (bridging-site adsorption) and the electronic structure between CO/Ni(111) and CO/Pd(110), we may expect similar large $\delta\omega$ for CO/Pd(110). The values for $\hbar\Omega$ and $\hbar\omega_0$ (T-mode) are ~240 meV and ~25 meV for CO/Pd(110) (*13*), and ~250 meV (*14*) and ~3.9 meV (*22*) He for CO on Cu at on-top position, respectively.

For CO on Pd(110), the second-order process gives $P \approx 10^{-9}$. To convert this to the hopping probability per tunneling electron, P should be multiplied by the probability that a tunneling electron excites the HF mode. This probability is determined by the change in

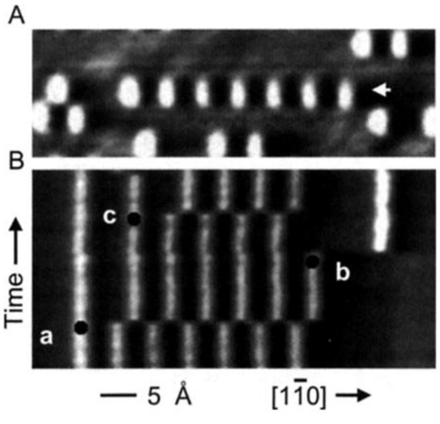

Fig. 4. (**A**) STM image (61 Å by 20 Å, I_{tunnel} = 1 nA, V_s = 50 mV) of CO on Pd(110); the ordered structure that has two times the periodicity of the substrate is formed by dosing CO at room temperature. (**B**) An example in which lateral motion is induced on a CO molecule at the edge of the 1D array that is imaged at the arrow mark of (A). The image is taken with the 1D dose-and-scan method and the *x* axis corresponds to 61 Å scanning and parallel to [1$\bar{1}$0]. Marks a, b, and c correspond to the points where tunneling electrons are dosed (V_s = 500 mV, I_{tunnel} = 7 nA and 1 s). At mark a, six molecules are shifted together to their right by single Pd lattice while the target molecule is left at its original position. The target molecule alone moves to right at mark b. At mark c, a simultaneous shift of the group of CO molecules can be observed again.

tunneling conductance, $\Delta\sigma/\sigma$, measured by inelastic tunneling spectroscopy. We have $\Delta\sigma/\sigma \sim 0.015$ for both CO/Cu (*14*) and CO/Pd(110), so that the hopping probability per tunneling electron should be 10^{-11}, which is of the same order of magnitude as the experimental results. From the first-order process, we also estimate a similar contribution to the hopping probability. The situation is markedly different for CO/Cu(110): the magnitude of $\delta\omega$ is much smaller, and n and n_0 are much greater than for CO/Pd(110). These differences make the transition much more difficult. For CO/Cu (110), we estimate $P \approx 10^{-26}$ for the second-order process and $P \approx 10^{-53}$ for the first-order process.

The results for tunneling-induced lateral motion of adsorbates presented above should open ways for further investigation. We show an example in Fig. 4 where lateral motion is induced on a CO molecule at the edge of an 1D array on Pd(110) at 4.8 K. The array is formed by dosing a submonolayer of CO at room temperature before the sample is cooled to 4.8 K. In this process, the CO molecules spontaneously form an ordered structure that has two times the periodicity of the substrate along the $[1\bar{1}0]$ direction (*23*) (Fig. 4A). We applied the 1D dose-and-scan method on the array of seven molecules at the arrow of Fig. 4A. With the dosing of electrons at mark "a" and "c" in Fig. 4B, a group of CO molecules are shifted simultaneously to the right, leaving the target molecule at its original position. The ability to shift an array of adsorbates is one of the fundamental requirements for the proposed atom relay devices (*24*). More generally, we believe that the manipulation of adsorbates by inducing their lateral hopping through dosing of tunneling electrons, may be a useful tool in nanotechnology and for basic research in surface dynamics.

References and Notes

1. G. Fedorus *et al.*, *Surf. Sci.* **251–252**, 846 (1991).
2. H. J. Jansch, J. Xu, J. T. Yates Jr., *J. Chem. Phys.* **99**, 721 (1993).
3. P. Avouris, *Acc. Chem. Res.* **18**, 95 (1995).
4. T. C. Shen *et al.*, *Science* **268**, 1590 (1995).

→ B. C. Stipe *et al.*, *Phys. Rev. Lett.* **78**, 4410 (1997).

6. B. C. Stipe, M. A. Rezaei, W. Ho, *Science* **279**, 1907 (1998).

→ ———, *Phys. Rev. Lett.* **81**, 1263 (1998).

8. The STM images reported here were taken at 4.8 K with a commercial STM (Omicron LT) in ultrahigh vacuum. The Pd(110) and Cu(110) were cleaned with a standard procedure described previously. The molecules of CO are dosed on the surface through a dosing tube located near the sample surface.
9. H. Kato, H. Okuyama, S. Ichihara, M. Kawai, J. Yoshinobu, *J. Chem. Phys.* **112**, 1925 (2000).
10. R. Raval, S. Haq, M. A. Harrison, G. Blyholder, D. A. King, *Chem. Phys. Lett.* **167**, 391 (1990).
11. N. Kitamura, M. G. Lagally, M. B. Webb, *Phys. Rev. Lett.* **71**, 2082 (1993).
12. The dosing event was executed with fixed tunneling current (7 nA) and the dosing period (1 s) for all applied voltages. The hopping probability was defined as the number of events in which the change of the bonding site occurs out of the total number of dosing events. We do not know exactly when the hopping occurs in the dosing period of 1 s. Thus, the remaining time after the event is a dead-time that makes the probability smaller. However, since the probability per event was chosen to be <0.1, the error is <5% of the value shown in the figure.
13. H. Kato, M. Kawai, J. Yoshinobu, *Phys. Rev. Lett.* **82**, 1899 (1999).

→ L. J. Lauhon, W. Ho, *Phys. Rev. B* **60**, R8525 (1999).

15. Again, the error bar of 5% should be considered as due to the dead-time effect.
16. B. G. Briner, M. Doering, H. P. Rust, A. M. Bradshaw, *Science* **278**, 257 (1997).
17. For details, see B. N. J. Persson, H. Ueba, *Surf. Sci.*, in press.
18. E. Schweizer *et al.*, *Surf. Sci.* **213**, 49 (1989).
19. T. A. Germer, J. C. Stephenson, E. J. Heilweil, R. R. Cavanagh, *J. Chem. Phys.* **101**, 1704 (1994).
20. M. Trenary, K. J. Uram, F. Bozso, J. T. Yates Jr., *Surf. Sci.* **146**, 269 (1984).
21. B. N. J. Persson, R. Ryberg, *Phys. Rev. Lett.* **54**, 2119 (1985).
22. J. Ellis, J. P. Toennies, G. Witte, *J. Chem. Phys.* **102**, 5059 (1995).
23. T. Komeda, Y. Kim, M. Kawai, *Jpn. J. Appl. Phys. Part 1* **40**, 4403 (2001).
24. Y. Wada, T. Uda, M. Lutwyche, S. Kondo, S. Heike, *J. Appl. Phys.* **74**, 7321 (1993).

25. Financial support was provided (in part) by the Grant-in-Aid for Scientific Research on Priority Areas "Surface Chemistry of Condensed Molecules" from the Japanese Ministry of Education, Culture, Sports, Science and Technology.

14 December 2001; accepted 12 February 2002

Laser-Induced Selectivity for Dimerization Versus Polymerization of Butadiene Under Pressure

Margherita Citroni,[1] Matteo Ceppatelli,[1] Roberto Bini,[1,2]* Vincenzo Schettino[1,2]

The pressure-induced chemical reaction of liquid butadiene was studied by Fourier transform infrared spectroscopy in a diamond anvil cell. Dimerization was found to occur above 0.7 gigapascal, giving vinylcyclohexene according to a cyclo-addiction reaction and only a trace amount of polybutadiene forms. By irradiating the high-pressure sample with a few milliwatts of the 488-nanometer argon$^+$ laser line, the dimerization was completely inhibited, and the rapid formation of pure *trans*-polybutadiene was observed. The use of different excitation wavelength allows us to emphasize the selectivity of the process and to identify the active role of the 2^1A_g state in this pressure- and laser-induced chemical reaction.

The outcomes of chemical reactions depend not only on energetics but on how molecules are oriented before reaction. In solution, steric effects can be used to favor particular orientations of reactants to guide reactivity and stereochemistry, and surface effects, whether exerted by heterogeneous catalysts or enzyme pockets, can also favor particular orientations of reactants. In the solid-state reactions, crystal lattices offer an even greater degree of geometrical constraint of reactants, but there are few examples of controlling reaction conditions (such as temperature and pressure) to select different reaction pathways. Chemical transformations occurring in molecular crystals at high pressure have been reported in a few cases (*1–9*) . Recently, we have also shown that at high pressure, laser irradiation and photochemical effects are a further effective regulatory tool of the reaction mechanism with the twofold effect of changing the pure pressure-induced reaction pathway and lowering the reaction pressure (*5*, *8*). This makes high-pressure reactions an appealing preparation method for large-volume applications. Here, we used geometrical constraints to induce selective chemical reactivity by applying ultrahigh pressures with a diamond anvil cell (DAC), thus varying the relative distances and orientations between molecules, and selective laser irradiation to control excitation. By simply balancing these two parameters, we were able to induce and fully control the quantitative transformation of liquid butadiene to a simple dimer (vinylcyclohexene) or to a highly stereoregular polymer (*trans*-polybutadiene).

We were interested in studying *trans*-butadiene, an unsaturated very reactive molecule, because it can give rise to a variety of reaction products. Butadiene is also extremely unstable at ambient conditions, dimerization being the main reaction pathway (*10*). The dimerization is a second-order cyclo-addition reaction. Three

---

[1] Dipartimento di Chimica dell'Università di Firenze, Polo Scientifico, Via della Lastruccia 3, I-50019 Sesto Fiorentino, Firenze, Italy. [2] LENS, European Laboratory for Non-linear Spectroscopy and INFM, Polo Scientifico, Via Carrara 1, I-50019 Sesto Fiorentino, Firenze, Italy.

*To whom correspondence should be addressed. E-mail: bini@srv.chim.unifi.it